A 3-D Perfectly Matched Medium by Coordinate Stretching and Its Absorption of Static Fields †

Weng Cho Chew and William H. Weedon
Electromagnetics Laboratory
Department of Electrical and Computer Engineering
University of Illinois, Urbana, IL 61801

Apo Sezginer
Schlumberger-Doll Research
Old Quarry Road
Ridgefield, CT 06877

Key Terms: Maxwell's equations, coordinate stretching, perfectly matched layer, finite difference time domain, massively parallel computer, static field absorbing boundary condition.

ABSTRACT—A modified set of Maxwell's equations is presented that includes complex coordinate stretching along the three Cartesian coordinates. The added degrees of freedom in the modified Maxwell's equations allow the specification of absorbing boundaries with zero reflection at all angles of incidence and all frequencies. The modified equations are also related to the perfectly matched layer that was presented recently for 2-D wave propagation. We have demonstrated that absorbing material boundary conditions are of particular interest for finite difference time domain (FDTD) computations on a single-instruction multiple-data (SIMD) massively parallel supercomputer.

In addition, we will show that PML will absorb static field and can be used to truncate a finite-difference mesh for electrostatic and magnetostatic simulations.

1. Introduction

The finite difference time domain method [1, 2] is widely regarded as one of the most popular computational electromagnetics algorithms. Although FDTD is conceptually very simple and relatively easy to program, the method is actually quite efficient since it involves $O(N^{1.5})$ computational complexity in 2-D and $O(N^{1.33})$ computational complexity in 3-D [3]. In fact, FDTD can be considered an optimal algorithm since $O(N^{\alpha})$ numbers are produced in $O(N^{\alpha})$ operations.

FDTD is also ideally suited for implementation on a single-instruction multiple-data (SIMD) massively parallel computer. The reason is that the stencil operations that must be computed at each node of the space grid involve only nearest-neighbor interactions and may be implemented at a minimum communication cost [4]. A major challenge, however, is in implementing absorbing boundary conditions (ABCs) at the edges of the FDTD grid. On scalar and vector computers, these boundary conditions are typically computed using methods such as the Engquist-Majda [5], Mur [6], Liao [7] or Higdon [8] ABC. However, these methods are not ideal for parallel supercomputers since they all involve communication with many elements normal to the grid boundary, which can easily surpass the time spent computing core FDTD operations in the grid interior. Also, they do not allow for SIMD operation on a parallel machine without the use of masking.

An alternate method of implementing an ABC is to use a conventional absorbing material boundary [4, 9–14] . For SIMD parallel computation, these methods have the advantage that the ABC may be implemented with the same FDTD stencil operation as the interior nodes by modifying the conductivity material parameter at the edge of the FDTD grid. The disadvantage is that the reflection coefficient at the absorbing border is

† This work is supported by the Office of Naval Research under grant N000-14-89-J1286, the Army Research Office under contract DAAL03-91-G-0339, the National Science Foundation under grant NSF-ECS-92-24466, and NASA under grant NASA-NAG-2-871. Computer time is provided by the National Center for Supercomputer Applications at the University of Illinois, Urbana-Champaign.

Applied Computational Electromagnetics Symposium Digest, vol. 1, pp. 482-489, Monterey, California, March 1995.

zero only at normal incidence and is both angle and frequency dependent. Consequently, the absorbing material border region must be made quite large—typically 20–100 grid points along each edge in order to minimize reflections.

Recently, Berenger [15] suggested a more general method of implementing an absorbing material boundary condition. Berenger proposed a procedure for 2-D wave propagation whereby Maxwell's equations are generalized and added degrees of freedom are introduced. The added degrees of freedom allow the specification of absorbing borders with zero reflection coefficient at all angles of incidence and all frequencies. Moreover, the generalized Maxwell's equations reduce to the familiar Maxwell's equations as a special case and hence the same generalized equations can be used to propagate fields in both the interior region and absorbing region. Although the interface between the interior region and the absorbing boundary is reflectionless, there is still a reflection from the edge of the grid. The advantage of using Berenger's procedure is that much larger conductivity values may be specified in the absorbing region, leading to a drastic reduction in the number of grid points required for the absorbing boundary.

A formulation similar to the Berenger idea has been derived for 3-D wave propagation from first principles using a coordinate stretching approach [16]. The advantage of the new method is for SIMD parallel computation. The method is validated with 3-D FDTD numerical computations on a Thinking Machines Corporation Connection Machine CM-5.

2. Modified Maxwell's Equations

For a general medium, we define the modified Maxwell's equations in the frequency domain, assuming $e^{-i\omega t}$ time dependence, as

$$\nabla_e \times \boldsymbol{E} = i\omega\mu\boldsymbol{H} \tag{1}$$

$$\nabla_h \times \boldsymbol{H} = -i\omega\epsilon\boldsymbol{E} \tag{2}$$

$$\nabla_h \cdot \epsilon\boldsymbol{E} = \rho \tag{3}$$

$$\nabla_e \cdot \mu\boldsymbol{H} = 0 \tag{4}$$

where

$$\nabla_e = \hat{x}\frac{1}{e_x}\frac{\partial}{\partial x} + \hat{y}\frac{1}{e_y}\frac{\partial}{\partial y} + \hat{z}\frac{1}{e_z}\frac{\partial}{\partial z} \tag{5}$$

$$\nabla_h = \hat{x}\frac{1}{h_x}\frac{\partial}{\partial x} + \hat{y}\frac{1}{h_y}\frac{\partial}{\partial y} + \hat{z}\frac{1}{h_z}\frac{\partial}{\partial z}. \tag{6}$$

In the above, e_i, h_i, $i = x, y, z$ are coordinate-stretching variables that stretch the x, y, z coordinates for ∇_e and ∇_h. For a plane wave, we can show that for a homogeneous medium, this gives the dispersion relation

$$\omega^2\mu\epsilon = \boldsymbol{k}_e \cdot \boldsymbol{k}_h \tag{7}$$

where $\boldsymbol{k}_e = \hat{x}\frac{k_x}{e_x} + \hat{y}\frac{k_y}{e_y} + \hat{z}\frac{k_z}{e_z}$ and $\boldsymbol{k}_h = \hat{x}\frac{k_x}{h_x} + \hat{y}\frac{k_y}{h_y} + \hat{z}\frac{k_z}{h_z}$, or

$$\kappa^2 = \frac{1}{e_x h_x}k_x^2 + \frac{1}{e_y h_y}k_y^2 + \frac{1}{e_z h_z}k_z^2 \tag{8}$$

where $\kappa^2 = \omega^2\mu\epsilon$. Equation (8) is the equation of an ellipsoid in 3-D and is satisfied by [16]

$$k_x = \kappa\sqrt{e_x h_x}\sin\theta\cos\phi, \tag{9}$$

$$k_y = \kappa\sqrt{e_y h_y}\sin\theta\sin\phi, \tag{10}$$

and

$$k_z = \kappa\sqrt{e_z h_z}\cos\theta. \tag{11}$$

Note that when e_i, h_i, $i = x, y, z$ are complex, the wave in the x, y, and z directions are attenuative and can be independently controlled. Under the matching condition, $e_x = h_x$, $e_y = h_y$, and $e_z = h_z$, we have $|\boldsymbol{k}_e|^2 = |\boldsymbol{k}_h|^2 = \kappa^2$. The wave impedance is then given by

$$\eta = \frac{|\boldsymbol{E}|}{|\boldsymbol{H}|} = \frac{|\boldsymbol{k}_h|}{\omega\epsilon} = \sqrt{\frac{\mu}{\epsilon}}, \tag{12}$$

irrespective of the values for $e_i, i = x, y, z$ and the direction of propagation.

3. Single Interface Problem

Assume that a plane wave is obliquely incident on the interface $z = 0$. Furthermore, we may assume that the plane wave is of arbitrary polarization. The incident field may be decomposed into a sum of two components, one with electric field transverse to z (TE^z) and the other with magnetic field transverse to z (TM^z).

We can derive their reflection and transmission coefficients as [16]

$$R^{\mathrm{TE}} = \frac{k_{1z}e_{2z}\mu_2 - k_{2z}e_{1z}\mu_1}{k_{1z}e_{2z}\mu_2 + k_{2z}e_{1z}\mu_1} \tag{13}$$

and

$$T^{\mathrm{TE}} = \frac{2k_{1z}e_{2z}\mu_2}{k_{1z}e_{2z}\mu_2 + k_{2z}e_{1z}\mu_1}. \tag{14}$$

Similarly, we have

$$R^{\mathrm{TM}} = \frac{k_{1z}h_{2z}\epsilon_2 - k_{2z}h_{1z}\epsilon_1}{k_{1z}h_{2z}\epsilon_2 + k_{2z}h_{1z}\epsilon_1} \tag{15}$$

and

$$T^{\mathrm{TM}} = \frac{2k_{1z}h_{2z}\epsilon_2}{k_{1z}h_{2z}\epsilon_2 + k_{2z}h_{1z}\epsilon_1}. \tag{16}$$

4. A Perfectly Matched Interface

The phase matching condition requires that $k_{1x} = k_{2x}$ and $k_{1y} = k_{2y}$, or

$$\kappa_1\sqrt{e_{1x}h_{1x}}\sin\theta_1\cos\phi_1 = \kappa_2\sqrt{e_{2x}h_{2x}}\sin\theta_2\cos\phi_2 \tag{17}$$

and

$$\kappa_1\sqrt{e_{1y}h_{1y}}\sin\theta_1\sin\phi_1 = \kappa_2\sqrt{e_{2y}h_{2y}}\sin\theta_2\sin\phi_2 \tag{18}$$

where $\kappa_1 = \omega\sqrt{\mu_1\epsilon_1}$ and $\kappa_2 = \omega\sqrt{\mu_2\epsilon_2}$. For a perfectly matched medium, we choose $\epsilon_1 = \epsilon_2$, $\mu_1 = \mu_2$, $e_x = h_x$ and $e_y = h_y$. Equations (17) and (18) become

$$e_{1x}\sin\theta_1\cos\phi_1 = e_{2x}\sin\theta_2\cos\phi_2 \tag{19}$$

and

$$e_{1y}\sin\theta_1\sin\phi_1 = e_{2y}\sin\theta_2\sin\phi_2. \tag{20}$$

If we now choose $e_{1x} = e_{2x}$ and $e_{1y} = e_{2y}$, then $\theta_1 = \theta_2$, $\phi_1 = \phi_2$ and we can show that both $R^{\mathrm{TE}} = 0$ and $R^{\mathrm{TM}} = 0$ for all angles of incidence and all frequencies.

If region 1 is a vacuum, then $\mu = \mu_0$, $\epsilon = \epsilon_0$, and

$$(e_{1x}, e_{1y}, e_{1z}, h_{1x}, h_{1y}, h_{1z}) = (1, 1, 1, 1, 1, 1). \tag{21}$$

In order to have a lossy region 2 with no reflections at the region 1/region 2 interface, we choose

$$(e_{2x}, e_{2y}, e_{2z}, h_{2x}, h_{2y}, h_{2z}) = (1, 1, s_2, 1, 1, s_2) \tag{22}$$

where s_2 is a complex number. In this case,

$$k_{1x} = k_{2x} = \kappa_0 \sin\theta \cos\phi \tag{23}$$

$$k_{1y} = k_{2y} = \kappa_0 \sin\theta \sin\phi \tag{24}$$

$$k_{1z} = \kappa_0 \cos\theta \tag{25}$$

$$k_{2z} = \kappa_0 s_2 \cos\theta \tag{26}$$

where $\kappa_0 = \omega\sqrt{\mu_0\epsilon_0}$. If $s_2 = s_2' + is_2''$, the wave will attenuate in the z direction. This kind of interface is useful for building material ABCs in a FDTD simulation.

In realistic simulation, we will have to choose $s_2'' \sim \frac{1}{\omega}$. Hence, when the frequency goes to zero, k_{2z} above becomes a purely imaginary number. Therefore, it attenuates static fields as well.

5. Modified Equations in the Time Domain

For the general case of a matched medium, we let $e_x = h_x = s_x$, $e_y = h_y = s_y$ and $e_z = h_z = s_z$. Next, we let $s_x = 1 + i\sigma_x/\omega\epsilon$, $s_y = 1 + i\sigma_y/\omega\epsilon$ and $s_z = 1 + i\sigma_z/\omega\epsilon$. Writing the equations in the time domain [16], we have

$$\mu\frac{\partial \boldsymbol{H}_{s_x}}{\partial t} + \frac{\sigma_x\mu}{\epsilon}\boldsymbol{H}_{s_x} = -\frac{\partial}{\partial x}\hat{x} \times \boldsymbol{E} \tag{27}$$

$$\mu\frac{\partial \boldsymbol{H}_{s_y}}{\partial t} + \frac{\sigma_y\mu}{\epsilon}\boldsymbol{H}_{s_y} = -\frac{\partial}{\partial y}\hat{y} \times \boldsymbol{E} \tag{28}$$

$$\mu\frac{\partial \boldsymbol{H}_{s_z}}{\partial t} + \frac{\sigma_z\mu}{\epsilon}\boldsymbol{H}_{s_z} = -\frac{\partial}{\partial z}\hat{z} \times \boldsymbol{E} \tag{29}$$

and

$$\epsilon\frac{\partial \boldsymbol{E}_{s_x}}{\partial t} + \sigma_x\boldsymbol{E}_{s_x} = \frac{\partial}{\partial x}\hat{x} \times \boldsymbol{H} \tag{30}$$

$$\epsilon\frac{\partial \boldsymbol{E}_{s_y}}{\partial t} + \sigma_y\boldsymbol{E}_{s_y} = \frac{\partial}{\partial y}\hat{y} \times \boldsymbol{H} \tag{31}$$

$$\epsilon\frac{\partial \boldsymbol{E}_{s_z}}{\partial t} + \sigma_z\boldsymbol{E}_{s_z} = \frac{\partial}{\partial z}\hat{z} \times \boldsymbol{H}. \tag{32}$$

Equations (27) – (32) described 3-D wave propagation in a perfectly matched medium. The wave propagation phenomenon described by these equations is very similar to that described by Maxwell's equations with the exception that attenuation may be controlled through the σ_x, σ_y and σ_z variables. The FDTD implementation of these equations on a Yee FDTD grid is straightforward. Absorbing boundaries at the edges of the simulation region may be created by choosing appropriate values of σ_x, σ_y and σ_z. Equations (27) – (32) may be seen to include Berenger's equations [15] as a subset for the 2-D TE or TM case.

6. Computer Simulation Results

To study the PML, we calculate the reflection coefficient for a plane wave incident with different values of k_x. The reflection coefficient is calculated for a step conductivity (σ_z) profile of 7 layers (with a metal backing) shown in Figure 1a. Figure 1b shows the reflection coefficient magnitude as a function of k_x/k_0 where $k_x = k_0$ corresponds to grazing incidence. Notice that the reflection coefficient magnitude is always 1 at grazing incidence. σ_{max} is the maximum value of σ_z for the step profile which increases in conductivity toward the metal backing. The overall reflection amplitude is smaller for increasing σ_{max}. Notice that the evanescent wave ($k_x > k_0$) are well absorbed.

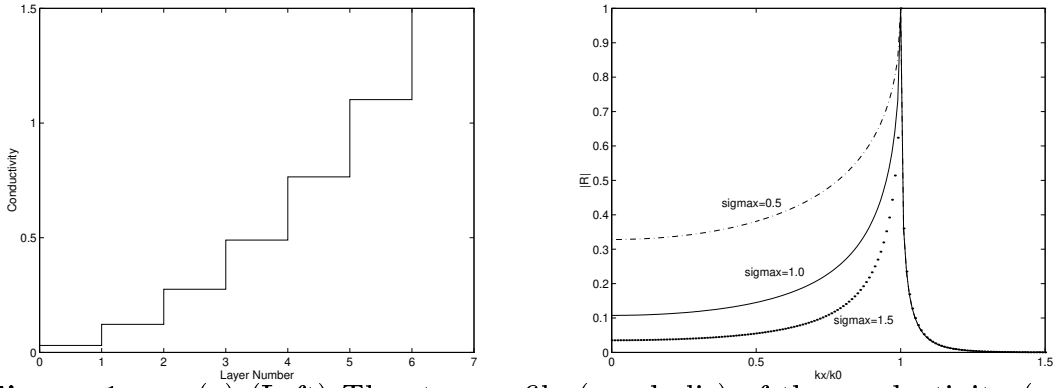

Figure 1: (a) (Left) The step profile (parabolic) of the conductivity (σ_z) used in the PML absorbing boundary. (b) (Right) The reflection coefficient magnitude as a function of a plane wave incident with different k_x's (x being the direction parallel to the interface) and different σ_{max}.

In Figure 2, we solve the Sommerfeld problem of a line source over a PML medium backed by a ground plane. The line source is located at the origin, with the first interface of the medium at a distance h_t below the line source. The observation point is located at (x, z). The amplitude of the field is plotted as a function of x for a fixed z. Notice that as σ_{max} increases, the result agrees with the ideal exact result, which is the case in the absence of the ground-plane-backed PML. Also, for large x, the discrepancy cannot be remedied by choices of σ_{max}. This is because the observer at larger x receives most of the reflected field through grazing reflection, where the PML medium does not absorb well.

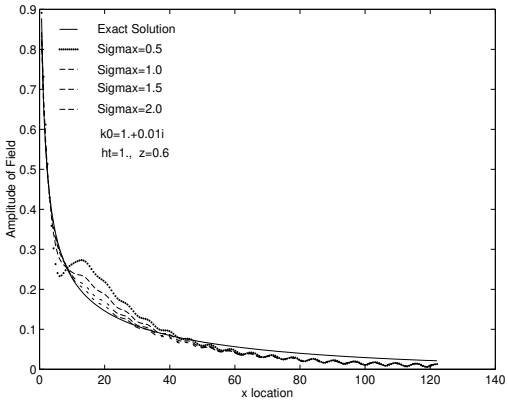

Figure 2: The field magnitude as a function of x for an electric line source over a PML medium backed by a ground plane for different σ_{max} in a seven layer parabolic profile. The thickness of each PML is 0.6.

In order to demonstrate the new method, a 3-D orthogonal grid FDTD algorithm was developed based on Equations (27) – (32). The FDTD algorithm was implemented as a SIMD code on the Thinking Machines Corporation Connection Machine CM-5. The algorithm operates very efficiently on the CM-5 because the FDTD stencil operations that need to be computed at each node involve only nearest-neighbor interactions. The communication operations resulting from the nearest-neighbor interactions are at a minimum cost.

The FDTD solution was solved in a cubic region of dimension $(N_x, N_y, N_z) = (128, 128, 32)$ grid points. The grid parameters chosen were $\Delta x = \Delta y = \Delta z = 2.5$ mm, $\Delta t = 4.5$ ps and $N_t = 512$ time steps were computed.

The infinitesimal electric dipole was simulated by exciting the E_y field in a single grid cell with the source pulse

$$J_y(t) = \frac{1}{\Delta x \Delta y \Delta z} \left[4(t/\tau)^3 - (t/\tau)^4 \right] e^{-t/\tau} \tag{33}$$

where $\tau = 1/4\pi f_0$ and a value of $f_0 = 1.0$ GHz was chosen. The dipole source was located at grid location $(n_x, n_y, n_z) = (91, 64, 16)$. The E_x and E_y fields were obtained by sampling the fields at grid location $(n_x, n_y, n_z) = (37, 91, 16)$.

The absorbing boundaries used for the FDTD simulation consisted of planar layers of thickness 8 grid points on all surfaces. Along the borders parallel to x axis, the value of σ_x was specified, while σ_y and σ_z were specified on the borders parallel to the y and z axis, respectively. The conductivity values were chosen with a parabolic taper.

The E_x field computed using both the analytic formulation and the FDTD algorithm are overlaid in Figure 3. The curves due to the analytic and numerical solutions are barely distinguishable, indicating excellent agreement.

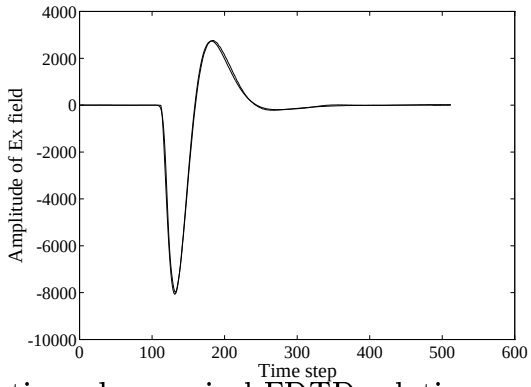

Figure 3: Analytic and numerical FDTD solution overlaid for the E_x field resulting from an infinitesimal electric dipole.

The CM-5 machine used to solve the FDTD problem is located at the National Center for Supercomputing Applications (NCSA) at the University of Illinois. The program was written in CM Fortran and compiled using CMF version 2.1. The CM-5 at the NCSA has 512 nodes with vector units. CPU times were determined by running the problem on 32, 64, 128 and 256 node partitions. For this problem, a total of 1.5 million unknown field quantities per time step

($128 \times 128 \times 32$ grid) were determined for 512 time steps. The CPU times are shown in Table 1.

In Figure 4, we show the absorption of electrostatic field by a PML medium. The plots are for the x-components of the electric field as a function of x due to a line of electric

Table 1: CPU times for FDTD Problem on CM-5

Nodes	CPU sec (Run 1, Run 2, Run 3, Avg.)
32	50.5, 50.2, 50.6; 50.4
64	29.9, 30.0, 30.0; 30.0
128	17.9, 18.4, 18.4; 18.2
256	12.4, 13.2, 12.7; 12.8

dipole pointing in the x-direction. The dotted line is the closed-form solution. The dotted-dashed line is the simulation with PML absorbing boundary condition. The solid line is the result from simulation using a modified impedance boundary condition. It is seen that the static field diminishes exponentially fast near the edge of the simulation region. In the simulation region of interest, the PML result agrees much better than the impedance boundary condition simulation when compared to the closed form solution.

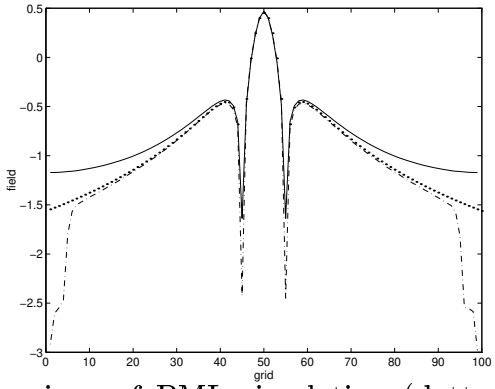

Figure 4: Comparison of PML simulation (dotted-dashed), impedance boundary condition simulation (solid) and closed form (dotted) for the x component of the electric field due to a line source of static electric dipole.

7. Conclusions

A modified set of Maxwell's equations have been introduced using complex coordinate stretching factors along the three Cartesian coordinate axis. This modification introduces additional degrees of freedom in Maxwell's equations such that absorbing boundaries may be specified with zero reflection coefficient at all frequencies and all angles of incidence. The formulation was shown to be related to the perfectly matched layer that was recently derived by Berenger for 2-D wave propagation. A 3-D FDTD algorithm was developed from the modified Maxwell's equations that uses the reflectionless absorbing interface property to implement radiation boundary conditions at the edges of the FDTD grid, and was implemented on the Connection Machine CM-5 and timing results were presented. This breakthrough in absorbing material boundary conditions allows EM scattering to be computed very efficiently on SIMD parallel computers. In addition, we show that PML does not absorb for waves at grazing incidence, but it could absorb static electromagnetic field.

References

[1] K. S. Yee, "Numerical solution of initial boundary value problems involving Maxwell's equations in isotropic media," *IEEE Trans. Antennas Propagat.*, vol. AP-14, pp. 302–307, 1966.

[2] A. Taflove, "Review of the formulation and applications of the finite-difference time-domain method for numerical modeling of electromagnetic wave interactions with arbitrary structures," *Wave Motion*, vol. 10, pp. 547–582, 1988.

[3] W. C. Chew, *Waves and Fields in Inhomogeneous Media.* New York: Van Nostrand, 1990.

[4] W. H. Weedon, W. C. Chew, and C. M. Rappaport, "Computationally efficient FDTD simulation of open-region scattering problems on the connection machine CM-5," in *IEEE Antennas and Propagation Society International Symposium Digest*, (Seattle, WA), June 19–24, 1994.

[5] B. Engquist and A. Majda, "Absorbing boundary conditions for the numerical simulation of waves," *Math. Computation*, vol. 31, pp. 629–651, 1977.

[6] G. Mur, "Absorbing boundary conditions for the finite-difference approximation of the time-domain electromagnetic field equations," *IEEE Trans. Electromag. Compat.*, vol. EMC-23, pp. 377–382, 1981.

[7] Z. P. Liao, H. L. Wong, B. P. Yang, and Y. F. Yuan, "A transmitting boundary for transient wave analysis," *Scientia Sinica. (Series A)*, vol. 27, no. 10, pp. 1063–1076, 1984.

[8] R. L. Higdon, "Numerical absorbing boundary conditions for the wave equation," *Math. Comput.*, vol. 49, pp. 65–90, 1987.

[9] I. Katz, D. Parks, A. Wilson, M. Rotenberg, and J. Harren, "Non-reflective free space boundary conditions for SGEMP codes," *Systems, Science and Software*, vol. SSS-R-76-2934, 1976.

[10] R. Holland and J. W. Williams, "Total-field versus scattered-field finite-difference codes: A comparative assessment," *IEEE Trans. Nuclear Sci.*, vol. NS-30, pp. 4583–4588, 1983.

[11] J.-P. Berenger in *Actes du Colloque CEM*, (Tregastel, France), 1983.

[12] C. Cerjan, D. Kosloff, R. Kosloff, and M. Reshef, "A nonreflecting boundary condition for discrete acoustic and elastic wave equations," *Geophysics*, vol. 50, pp. 705–708, 1985.

[13] R. Kosloff and D. Kosloff, "Absorbing boundaries for wave propagation problems," *J. Computational Physics*, vol. 63, pp. 363–376, 1986.

[14] C. M. Rappaport and L. Bahrmasel, "An absorbing boundary condition based on anechoic absorber for EM scattering computation," *J. Electromag. Waves Appl.*, vol. 6, no. 12, pp. 1621–1634, 1992.

[15] J.-P. Berenger, "A perfectly matched layer for the absorption of electromagnetic waves," *J. Computational Physics*, vol. 114, pp. 185–200, 1994.

[16] W. C. Chew and W. H. Weedon, "A 3d perfectly matched medium from modified maxwell's equations with stretched coordites," *Micro. Opt. Tech. Lett.*, vol. 7, pp. 599–604, 1994.